

## Assessment of Heavy Metal Pollution and Related Risks to Human Health – A Case of Angads Plain, Morocco

Oualid Boukich<sup>1,2\*</sup>, Rihab Ben-Tahar<sup>1,2</sup>, Nour-Elhouda Basraoui<sup>1,2</sup>,  
Elkhadir Gharibi<sup>3</sup>, Bouchra El Guerrouj<sup>1,2</sup>, Youssef Smiri<sup>1,2</sup>

<sup>1</sup> Laboratory for the Improvement of Agricultural Production, Biotechnology, and Environment, Faculty of Sciences, Mohammed First University, Oujda, Morocco

<sup>2</sup> Oriental Center of Water and Environment Sciences and Technologies, Mohammed First University, Oujda, Morocco

<sup>3</sup> Applied Chemistry and Environment Laboratory, Faculty of Sciences, Mohammed First University, Oujda, Morocco

\* Corresponding author's e-mail: [oualid.boukich@ump.ac.ma](mailto:oualid.boukich@ump.ac.ma)

### ABSTRACT

The present article assesses, for the first time, the level of heavy metal pollution, determines possible sources and evaluates the health risks associated with groundwater in the Angads plain in Morocco, by employing a combination of tools including indices, statistical multivariate techniques and models for health risk assessment. The findings revealed that the concentrations of several heavy metals (95.83% for As and 41.66% for Pb) were above the WHO limit values. The heavy metal pollution index (HPI) and the heavy metal evaluation index (HEI) revealed that all samples were fit for consumption. Health risks revealed that the hazard index (HI) values for dermal exposure were below the limit, while for oral exposure, 95.83% of samples were above the limit. In addition, the carcinogenic risk (CR) results revealed that there is a possibility of cancer development due to lifetime exposure to this groundwater.

**Keywords:** groundwater, trace metals, pollution indices, human health risk, Angads, Morocco.

### INTRODUCTION

Good quality drinking water is crucial to human health and environmental protection (Basraoui et al., 2024). Contaminated water represents a serious threat to aquatic ecosystems and human populations. Frequently, water quality deterioration is often due to inorganic and organic pollutants. In particular, heavy metals such as lead, nickel and chromium are a cause for concern (Rajmohan et al., 2022). These elements are characterized by their chemical stability, wide range of sources, persistence and high toxicity, as well as their capacity to accumulate in living organisms (Masoud et al., 2022). The pollution of aquatic systems by heavy metals is a growing global problem, exacerbated by demographic expansion and economic development.

Heavy metals in water can affect humans in a variety of ways (USEPA, 2014). Direct consumption of contaminated water, and ingestion of foods

and beverages prepared with this water, are the most common modes of exposure (USEPA, 2014). Other routes include skin absorption during bathing or showering, and inhalation of contaminated water particles. Globally, consumption of water contaminated with heavy metals has been associated with serious health problems, including bladder, lung and skin cancers, kidney disease, cardiovascular and neurological disorders, hyperpigmentation of the palm and hypertension (Kim et al., 2019; Egbueri, 2020; Bangotra et al., 2023).

Heavy metals enter water resources through a variety of anthropogenic and natural mechanisms. Natural processes include the decomposition of organic matter, rock erosion and atmospheric deposition (Wagh et al., 2018). However, human activities such as pesticide and fertilizer use, domestic and agricultural wastes, industrial discharges and mining significantly contribute to the heavy metal content of water (Mahjoub et al., 2024). Once in the aquatic environment, the

solubility of these metals, which determines their impact on water quality, is influenced by factors such as organic matter concentration, redox conditions and water pH (Ren et al., 2021).

A detailed understanding of trace element concentrations in water and their impact on health is crucial for optimal control and management of water resources. Assessing the health risks associated with water pollution makes it possible to quantify potential impacts and develop appropriate mitigation measures (Khan et al., 2023). This evaluation is frequently conducted employing chemometrics, an approach that relies primarily on mathematical or statistical principles to address the challenges associated with chemical pollution of water resources. Geospatial tools, such as inverse distance weighting models, is used to assess contaminant distribution and associated risks. In various parts of the world, researchers (Mohammadi et al., 2019; Shams et al., 2020; Egbueri, 2020; Rajmohan et al., 2022; Bangotra et al., 2023) have applied different mathematical, statistical and geospatial methodologies, such as pollution indices, multivariate statistical analyses, inverse distance weighting models and kriging, as well as health risk assessments, both non-carcinogenic and carcinogenic, to analyze water quality and the health risks associated with various trace elements in water.

Because of its location in arid and semi-arid regions, Morocco suffers significantly from the adverse impacts of climate change. The country has undergone a transition from water stress to water scarcity over the past two decades. This is reflected in more frequent and more severe periods of drought, as well as irregular and decreasing rainfall. These phenomena are slowing down the renewal of available water resources and increasing the country's vulnerability to water management. Currently, the average per capita water supply is considerably reduced, from 2,500 m<sup>3</sup> per year in the 1960s to just 650 m<sup>3</sup> in 2022 (RISS, 2022). This situation has led a large proportion of the population to turn to groundwater for their drinking and domestic water needs, as it represents the only available source in the study area. Despite this critical dependence, the quality of local groundwater has never been thoroughly assessed. This study represents the first attempt (1) to assess the distribution of trace metals in the Angads aquifer, (2) to evaluate the suitability of groundwater for consumption, (3) to assess the level of groundwater pollution using various indices, (4) identify

the source of trace elements using multivariate statistical analyses, and (5) assess health risks due to exposure to trace metals, by mapping these areas using geographic information systems. The study includes the creation of groundwater quality maps, an innovative approach in the research area. These results will provide fundamental information on the distribution and status of trace metals, essential for the management and conservation of groundwater resources.

## MATERIALS AND METHODS

### Study area description

The Angad plain, located in north-eastern Morocco (1°45'00"/2°4'00"W, 34°39'00"/34°54'00"N), has a surface area of 460 km<sup>2</sup> and a population of around 551767, contributing to the specificity of its demographic and socio-economic environment (GPHC, 2014). The plain is located in an agricultural area, where it plays a key role in the development of the region's social economy. The area under study is defined by a Mediterranean semi-arid to arid climate, characterized by mild to cold, hot summers and rainy winters. The average annual minimum and maximum temperatures in the area are 10.1 °C and 27.4 °C, respectively. Over 264.5 mm of precipitation falls in the region each year (MWBA, 2023). The groundwater system has multiple discharge points, including various domestic and agricultural activities. Domestic activities encompass household water use for drinking, bathing, and cleaning. Agricultural activities involve irrigation for crop cultivation, animal watering, and other farming needs.

### Geology and hydrogeology

The Angad plain is a vast depression stretching from east to west, and its fill consists of two distinct litho-stratigraphic units separated by an angular or gully unconformity. The first, of lower marine origin, is made up of conglomerates and limestones, followed by blue marls topped by yellow marls. Approaching the edges of the depression, these same rock types evolve into reef or volcano-detrital facies interbedded with basalt flows (Aqil et al., 2010). The assemblage contains fossils that give it an age ranging from Upper Tortonian to Messinian. The second set,

higher up and of detritic or volcano-detritic origin, is continental and devoid of fossils, with interbedded basalt flows. The two formations rest in angular unconformity on a Mesozoic bedrock. Hydrogeologically, two types of water table can be identified in the region: a phreatic water table in the Plio-Quaternary formations and a deep captive water table in the Jurassic dolomitic limestones and dolomites (Boughriba et al., 2010). The water table flows from south to north through the post-Miocene terrain, resting on an impermeable bedrock of Upper Miocene marls. They also act as an impermeable cover for the deep-water table. Lateral heterogeneity of facies, such as cinerites, basaltic ashes, compact or fissured basalts, silts, gravels, conglomerates, and lacustrine limestones, characterizes the diversity of aquifer layers in the water table (Lahrach et al., 2006). The groundwater flow direction is from southwest to northeast, and the main source of groundwater recharge is attributed to precipitation (Zarhloule et al., 2010). Groundwater levels range from 15 to 87 meters below the earth’s surface (Boughriba et al., 2010).

**Sample collection, and analysis**

24 groundwater samples were taken at various boreholes around the research area (Figure 1). To avoid sampling stagnant groundwater, samples were taken after 15 to 20 minutes of pumping. They were then filtered through filters (0.45 μm) and placed in bottles cleaned with distilled water and rinsed several times with the sample. 65% HNO<sub>3</sub> was used to acidify the samples immediately on site after collection, until the pH was stabilized below 2. The samples were then stored in a freezer at 4°C and transported to the laboratory for analysis. pH and electrical conductivity (EC) values were measured in the field during sampling, with a portable pH/EC meter. In addition, heavy metals (Al, As, Cr, Cu, Fe, Ni, Pb and Zn) were analyzed using an ICP-OES (Ultima expert) at the National Center for Scientific and Technical Research (CNRST) in Rabat.

**Pollution indices**

Various indices of pollution were employed to evaluate groundwater quality, detect any pollution and determine its potability. To calculate the heavy metal indices in various samples, the World Health Organization’s drinking water quality standards (WHO, 2017) were used (Table 1).

*Heavy metal pollution index*

Heavy metal pollution index (*HPI*) is a method for assessing the impact of heavy metal on water quality and potability (Sharma et al., 2022). Each metal’s weight and rating are used to calculate *HPI*. The weight is inversely proportional to each individual metal’s international drinking water guidelines, and the rate is an arbitrary number between 0 and 1. Equation 1 is used to calculate *HPI*.

$$HPI = \frac{\sum_{i=1}^n W_i Q_i}{\sum_{i=1}^n W_i} \tag{1}$$

where: the subindex of the *i*th element is *Q<sub>i</sub>* and the weighting unit index for the *i*th parameter is *W<sub>i</sub>* was computed by Equation 2.

$$W_i = \frac{1}{S_i} \tag{2}$$

where: *S<sub>i</sub>* is the permissible maximum value of *i*th element, and the calculation formula for *Q<sub>i</sub>* is shown in Equation 3.

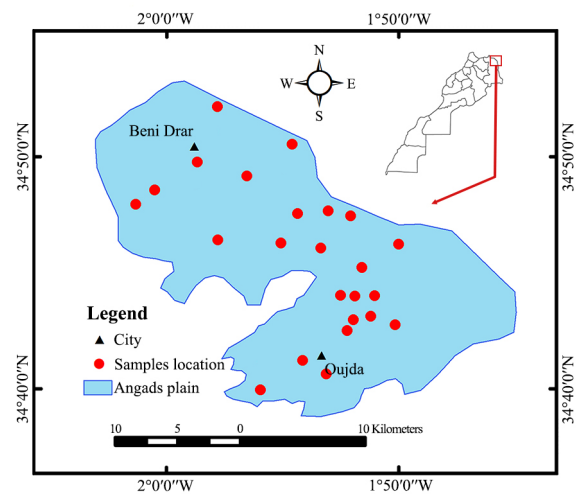


**Figure 1.** Groundwater sampling sites and study area location

**Table 1.** WHO recommended limits (μg/L) and percentage of samples exceeding the limits

Parameter	Al	As	Cr	Cu	Fe	Ni	Pb	Zn
WHO	200	10	50	2000	300	70	10	3000
%Fit	100	4.17	100	100	100	100	58.34	100
%Unfit	0	95.83	0	0	0	0	41.66	0

$$Q_i = \sum_{i=1}^n \frac{|M_i - I_i|}{(S_i - I_i)} \times 100 \quad (3)$$

where:  $I_i$  is the ideal or intended value, and  $M_i$  is the level of heavy metal.  $HPI$  is classified as shown in Table 2.

**Heavy metal evaluation index**

Heavy metal evaluation index ( $HEI$ ) provides a thorough evaluation of the overall water quality in terms of heavy metals pollution (Singh et al., 2020) and were calculated using Equation 4.

$$HEI = \sum_{i=1}^n \frac{M_i}{S_i} \quad (4)$$

where:  $M_i$  represents the concentration of heavy metal and  $S_i$  the permissible maximum value of the  $i$ th element.  $HEI$  is classified as shown in Table 2.

**Health risk assessment**

To evaluate the health impact of exposure to heavy metals through dermal absorption and oral, a study was conducted on two distinct age groups: adults and children. Health risk was assessed according to the toxicity of the metals, classifying them as non-carcinogenic or carcinogenic.

**Non-carcinogenic health risk**

The oral and dermal exposure of heavy metals found in the research area’s groundwater were used to quantify the non-carcinogenic health risks to humans. Hazard quotients ( $HQ$ ) and the hazard index ( $HI$ ) were assessed in this study to determine the possible non-carcinogenic health risk associated with oral and dermal exposure to groundwater. The US Environmental Protection Agency’s Equations 5 and 6 were used to determine the chronic daily intake ( $CDI$ ) of heavy metal by oral and dermal adsorption of water to humans.

$$CDI_{oral} = \frac{C_i \times IR \times EF \times ED}{BW \times AT} \quad (5)$$

$$CDI_{dermal} = \frac{C_i \times SA \times K_p \times ET \times EF \times ED \times CF}{BW \times AT} \quad (6)$$

where:  $C_i$  denotes the concentration of the  $i$ th heavy metal in water and  $IR$  refers to the rate of oral water consumption; exposure frequency and duration are symbolized by  $EF$  and  $ED$ , respectively;  $BW$  represents the average body weight;  $AT$  stands for the average exposure time;  $SA$  is the skin contact area;  $K_p$  is the skin adsorption parameter;  $ET$  is the exposure time;  $CF$  is the conversion factor. Table 3 shows values of the parameters used to evaluate the non-carcinogenic risk in this research.

The  $HQ$  is obtained by dividing the average  $CDI$  of a heavy metal by the reference dose ( $RfD$ ). To evaluate the  $HQ$  of heavy metals through oral and dermal exposure, Equations 7 and 8 were used.

$$HQ_{oral} = \frac{CDI_{oral}}{RfD_{oral}} \quad (7)$$

$$HQ_{dermal} = \frac{CDI_{dermal}}{RfD_{dermal}} \quad (8)$$

where:  $RfD_{oral}$  and  $RfD_{dermal}$  represents chronic reference dose. The reference dose values are presented in Table 4.

The  $HI$  is then determined by summing all  $HQs$  of examined parameters for both pathways, as illustrated in Equations 9 and 10.

$$HI_{oral} = \sum_{i=1}^n HQ_{oral} \quad (9)$$

$$HI_{dermal} = \sum_{i=1}^n HQ_{dermal} \quad (10)$$

The threshold value was established at 1 to evaluate the possible non-carcinogenic health hazards associated with various heavy metals found in waters. A  $HI$  value of less than 1 indicates that exposed people may not be anticipated to suffer from harmful health effects. Conversely, an  $HI$  score  $> 1$  indicates that there may be non-carcinogenic health hazards for the local population in the research region (Bangotra et al., 2023).

**Carcinogenic risks**

The cancer risks ( $CR$ ) calculates the life-time risk of developing cancer as a result of

**Table 2.** Classification of indices for water assessment

Indices	Category	Degree of pollution	References
HPI	<5	Low	Mthembu et al., 2022
	5–10	Medium	
	>10	High	
HEI	<9	Low	Singh et al., 2020
	9–18	Medium	
	>18	High	

**Table 3.** Parameter used to calculate the non-carcinogenic human health risk (USEPA, 2011)

Parameter	Unit	Values
IR	L/day	0.78 (children), 2.5 (adults)
EF	Days/year	365
ED	Year	6 (children), 70 (adults)
BW	kg	15 (children), 70 (adults)
AT	Day	ED × 365
SA	cm <sup>2</sup>	6600 (children), 18000 (adults)
K <sub>p</sub>	cm/hour	Al, As, Cu, Fe: 0.001; Cr: 0.002; Pb: 0.0001; Ni: 0.0002; Zn: 0.0006
ET	Hour/event	1 (children), 0.58 (adults)
CF	L/cm <sup>3</sup>	0.001

**Table 4.** Reference dose and cancer slope factor of heavy metals

Factor	Al	As	Cr	Cu	Fe	Ni	Pb	Zn
RfD <sub>oral</sub>	0.025 <sup>a</sup>	0.0003 <sup>a</sup>	0.003 <sup>a</sup>	0.04 <sup>a</sup>	0.3 <sup>a</sup>	0.02 <sup>a</sup>	1.4 <sup>a</sup>	0.3 <sup>a</sup>
RfD <sub>dermal</sub>	0.2 <sup>a</sup>	0.000123 <sup>a</sup>	0.000015 <sup>a</sup>	0.012 <sup>a</sup>	0.045 <sup>a</sup>	0.0054 <sup>a</sup>	0.00042 <sup>a</sup>	0.06 <sup>a</sup>
CSF <sub>oral</sub>		1.5 <sup>b</sup>	0.5 <sup>b</sup>			0.91 <sup>c</sup>	0.0085 <sup>c</sup>	
CSF <sub>dermal</sub>		3.66 <sup>b</sup>	0.5 <sup>b</sup>					

**Note:** <sup>a</sup>USEPA, 2014, <sup>b</sup>Yuan et al., 2023, <sup>c</sup>Shil and Singh, 2019.

daily exposure to a particular level of carcinogenic metals by multiplying the *CDI* and cancer slope factor (*CSF*) (USEPA, 2011; Mohammadi et al., 2019). Equations 11 and 12 was used to calculate the CR for oral and dermal absorption pathways, respectively. The oral and dermal cancer slope factor are presented in Table 3.

$$CR_{oral} = CDI_{oral} \times CSF_{oral} \quad (11)$$

$$CR_{dermal} = CDI_{dermal} \times CSF_{dermal} \quad (12)$$

where: *CSF*<sub>oral</sub> and *CSF*<sub>dermal</sub> represents cancer slope factor.

The total cancer risk (*TCR*) represents the cumulative carcinogenic health risks associated with oral and dermal exposure. These risks were assessed using the following Equation 13.

$$TCR = CR_{oral} + CR_{dermal} \quad (13)$$

Values <10<sup>-6</sup> are classified as low risk, between 10<sup>-6</sup> and 10<sup>-4</sup> as moderate risk, between 10<sup>-4</sup> and 10<sup>-3</sup> as high cancer risk, and >10<sup>-3</sup> as extremely high cancer risk (USEPA, 2011).

### Multivariate analysis

Two statistical analytic techniques utilized to understand the origins and affecting factors are Pearson correlation matrix (PCM) and principal component analysis (PCA) (Alshehri et al., 2021). PCM was used to determine the relationship

between variables and their potential sources. PCA was applied to identify the principal components according to their loading factors, highlighting the contribution of significant variables to groundwater pollution.

### Spatial analysis

ArcGIS 10.3 software was used to create spatial distribution maps, with the inverse distance weighted interpolation (IDW) method. IDW uses a deterministic model approach, where the unknown data are calculated using close points rather than distant ones. The spatial distribution of water quality has been extensively studied using the IDW interpolation approach (Bouaissa et al., 2022; Biswas et al., 2023).

## RESULTS AND DISCUSSION

Table 5 present descriptive statistics for the physicochemical parameters analyzed. In this aquifer, groundwater pH is mainly neutral ranging from 7.17 to 7.9 with a mean of 7.57. The EC values of groundwater samples ranged from 1261 to 5098 μS/cm, with a mean value of 2396.9 μS/cm. According to the mean concentrations in the groundwater samples, the concentration order of the metals decreasing as follow: Fe > Al > As

> Zn > Pb > Ni > Cr > Cu. Table 5 and Figure 2 present descriptive statistics for the trace metals analyzed and spatial distribution maps for these metals, respectively. The levels of groundwater trace metals found were compared with the recommended WHO guideline values (WHO, 2017). Aluminium (Al) concentrations ranged from 4.90 to 45.60 µg/l, with an average of 23.88 µg/l. Table 1 and Figure 2 show that 100% of samples are below WHO guide values and are therefore recommended for consumption. For Arsenic (As), groundwater concentrations ranged from 0.30 to 29.90 µg/l (mean of 17.31 µg/l). 95.83% of samples above the WHO limit, making them unsuitable for consumption (Table 1). The spatial distribution map shows that, according to As concentration, suitable well water is mainly found in the center of the study region (Figure 2). Chromium (Cr) concentrations in the study area ranged from 0.00 to 9.10 µg/l, with an average of 1.55 µg/l. Figure 2 shows that Cr concentration in all samples is below the WHO recommended potability limit. Copper (Cu) concentrations in groundwater varied from 0.00 to 1.50 µg/l, with mean of 0.24 µg/l. Table 1 and Figure 2 show that 100% of samples conform to the WHO standard and are fit for consumption. Iron (Fe) concentrations ranged from 3.70 to 269.90 µg/l, with an average of 44.07 µg/l. All samples were within recommended limits (Table 1). Nickel (Ni) concentrations ranged from 0.00 to 8.50 µg/l, with an average of 3.08 µg/l, and all samples were below the WHO recommended limit for drinking water (Table 1, Figure 2). Lead (Pb) concentrations ranged from 0.00 to 48.50 µg/l (mean of 11.45 µg/l). 41.66% of samples are not recommended for consumption as they surpass the WHO limit. Consumption of water containing high concentrations of Pb can lead to various health problems,

such as gastrointestinal disorders, neurological disorders and reduced lung function (WHO, 2017). As shown in Figure 2, groundwater values are low in the central region, while enrichment levels are noted in the vicinity of the study area. Zinc (Zn) concentrations range from 0.00 to 298.30 µg/l, with a mean of 16.10 µg/l. All samples are within WHO standard limits and therefore fit for consumption (Table 1).

Average concentrations of heavy metals were compared with those found in different parts of the world, to provide an insight into groundwater pollution in different regions (Table 6). Al content in groundwater samples is comparable to that of the other regions studied, except in the Kert basin where a very low concentration was found. The concentration of As in our study is higher than all the other countries cited, with the exception of the Bazman basin, where similar concentrations were found. Average Cr and Ni concentrations are lower than the Ben Taieb groundwater, with concentrations 13 times lower for Cr and 6 times lower for Ni. Groundwater from the Angads aquifer contains more Cu than that from the Kert basin. In comparison with the other studies mentioned, the results indicate that Cu content is very low, except in the Odisha plain in India, where the average Fe concentration is very high. All other regions show Fe levels in groundwater below the WHO recommended limit. Nayak and Nandimandalam (2023) reported that the high Fe concentrations in these waters may be due to salinization and microbial activity, which promotes the dissolution of Fe from source rocks. This study found higher Pb concentrations than all the other studies cited. The average Zn concentration detected was almost equal to that found in the Odisha plain in India, but lower than that detected in groundwater

**Table 5.** Statistics of pH, EC (µS/cm) and heavy metals (µg/L)

Specification	Min	Max	Mean
pH	7.17	7.90	7.57
EC	1261	5098	2396.9
Al	4.90	45.60	23.88
As	0.30	29.90	17.31
Cr	0.00	9.10	1.55
Cu	0.00	1.50	0.24
Fe	3.70	269.90	44.07
Ni	0.00	8.50	3.08
Pb	0.00	48.50	11.45
Zn	0.00	298.30	16.10

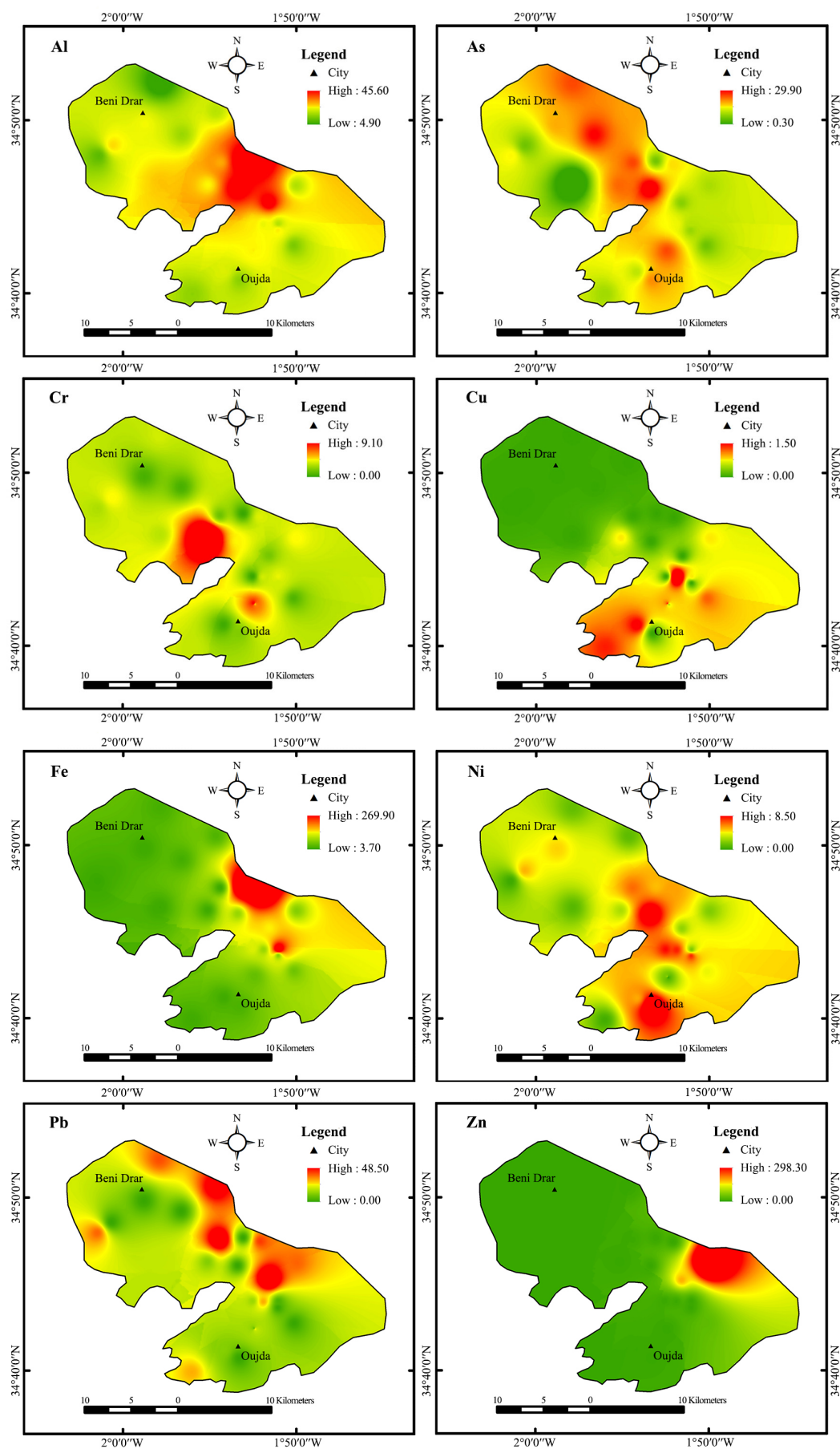


Figure 2. Distribution spatial of heavy metals

**Table 6.** Comparison of heavy metal concentrations with different regions of the world ( $\mu\text{g/L}$ )

Location	Al	As	Cr	Cu	Fe	Ni	Pb	Zn	References
Kert Basin, Morocco	0.042	–	0.001	0.044	0.065	0.018	0.001	0.11	Gueddari et al., 2021
Ben Taieb, Morocco	26.00		20.00	72.00	146.00	18.00	1.50	400.00	Gueddari et al., 2022
Saïs Plain, Morocco	–	0.64	3.82	630	120	–	0.67	770	Lotfi et al., 2020
Bazman basin, Iran	–	15.50	8.75	0.65	8.00	7.23	–	1.83	Rezaei et al., 2019
District Vehari, Pakistan	–	–	–	0.31	1.67	0.09	0.14	0.61	Khalid et al., 2020
Odisha plains, India	25.52	12.35	0.98	0.24	1511.2	10.46	–	17.85	Nayak and Nandimandalam, 2023
Huangpi District, China	–	1.37	1.59	3.00	57.43	1.24	0.18	45.44	Han et al., 2023
Angads aquifer	23.88	17.31	1.55	0.24	44.07	3.08	11.45	16.10	This study

from Ben Taieb, the Saïs plain and the Huangpi district in China. The highest levels of Cu and Zn were observed in the Saïs plain. Lotfi et al (2020) reported that these levels were due to industrial activities. Although the waters of the Kert basin have the lowest concentrations of heavy metals and are therefore of good quality. It is alarming to note that almost all the elements present in Morocco's groundwater are present in higher concentrations than in the other countries cited. This suggests a worrying level of groundwater contamination and the need to take appropriate action immediately.

### Trace metals pollution assessment

To detect any heavy metal pollution in the groundwater of the region, pollution indices, notably the *HPI* and *HEI*, were calculated. Table 7 presents the descriptive statistics for heavy metal pollution indices. The results show that *HPI* ranges from 0.16 to 1.03, with a mean of 0.49. According to these results, all groundwater samples are safe for drinking. In addition, *HEI* values range from 1.15 to 6.56, with a mean of 3.22. According

to *HEI* classification, all groundwater samples are classified as low pollution.

### Assessment of health risks

#### Non-carcinogenic health risks

Heavy metals can penetrate the human body by a variety of ways, including skin contact, as well as consumption of water and food, posing potential health risks (USEPA, 2014). This study focused on dermal and oral exposure for adults and children to assess health risks. Based on mean *HQ* values, it was found that As is the heavy metal to which adults and children are most exposed through oral ingestion, while Cr is the one to which they are most exposed through dermal ingestion. Cu, on the other hand, is the heavy metal to which both groups are least exposed, whether by ingestion or dermal contact. The average *HQ*<sub>oral</sub> value for both groups shows the following trend: As > Al > Cr > Ni > Fe > Zn > Pb > Cu, while the mean *HQ*<sub>dermal</sub> value shows the following trend: Cr > As > Pb > Fe > Zn > Al > Ni > Cu. For both groups, the mean *HQ*<sub>oral</sub> value for arsenic is greater than 1, indicating its negative impact

**Table 7.** Calculated HPI and HEI values

Sample ID	HPI	HEI	Sample ID	HPI	HEI	Sample ID	HPI	HEI
GW1	0.19	1.35	GW10	0.41	2.79	GW19	0.48	3.15
GW2	1.02	6.24	GW11	0.20	2.11	GW20	0.40	2.68
GW3	0.75	4.53	GW12	0.44	2.77	GW21	0.83	5.11
GW4	0.63	3.82	GW13	0.16	1.15	GW22	0.50	3.10
GW5	0.65	4.06	GW14	0.19	1.30	GW23	0.68	5.20
GW6	0.51	3.47	GW15	0.22	1.61	GW24	0.56	3.63
GW7	0.34	2.17	GW16	0.27	2.27	Min	0.16	1.15
GW8	1.03	6.56	GW17	0.36	2.34	Max	1.03	6.56
GW9	0.34	2.20	GW18	0.57	3.72	Mean	0.49	3.22



on human health and non-carcinogenic potential risks, such as respiratory, cardiovascular and neurological diseases. In contrast, the mean  $HQ_{\text{dermal}}$  values for all heavy metals, for both adults and children, are below 1, indicating a lower risk via the dermal exposure route.  $HQ_{\text{oral}}$  and  $HQ_{\text{dermal}}$  results show that  $HQ$  values for children are higher than for adults, suggesting that children are more vulnerable in the study area.  $HI_{\text{oral}}$  values range from 0.13 to 5.33 with a mean of 3.10 for children, and from 0.09 to 3.66 with an average of 2.13 for adults. In contrast,  $HI_{\text{dermal}}$  values ranged from 0.04 to 0.61 with a mean of 0.15 for children, and from 0.01 to 0.21 with a mean of 0.05 for adults. Compared with the  $HI$  critical limit, 2.2% of samples for adults and children did not exceed this limit, meaning they were safe for ingestion. For dermal use, all samples did not exceed the  $HI$  critical limit, revealing that they were low non-carcinogenic. The spatial distribution of  $HI$  for ingestion, for both groups, shows that the only sample presenting no risk is located in the center of the study area (Figure 3).

### Carcinogenic health risks

In this research, the elements As, Cr, Ni and Pb were considered to evaluate carcinogenic risk through  $CR$ . Risks associated with As and Cr were assessed for both exposure routes, while for Ni and Pb, only the oral route was considered. The  $TCR$  was calculated to estimate the cumulative carcinogenic risks of the metals studied for both exposure routes. The results of the total incremental lifetime cancer risk due to dermal and oral exposure to heavy metals in groundwater samples are presented in Table S3.  $CR_{\text{dermal}}$  values range from 1.1E-06 to 4.9E-05, with a mean value of 2.9E-05 for children, and from 3.6E-07 to 1.7E-05, with a mean value of 9.7E-06 for adults. In contrast,  $CR_{\text{oral}}$  values range from 1.1E-04 to 2.7E-03, with an average value of 1.5E-03 for children, and from 7.5E-05 to 1.9E-03, with an average value of 1.1E-03 for adults. Based on  $CR$  critical values, it was found that, for the oral route, 95.5% of groundwater samples for children and 28.9% for adults presented a very high carcinogenic risk, particularly of the liver,

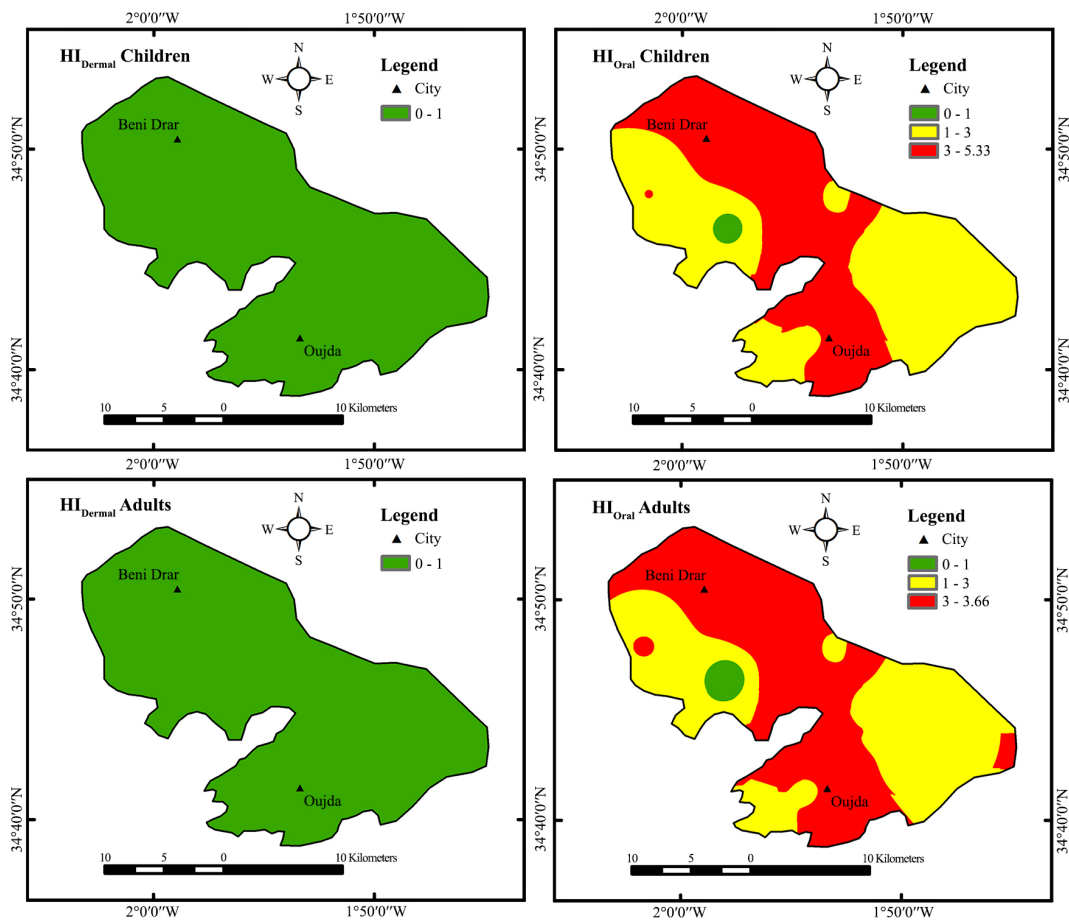


Figure 3. Distribution spatial of HI

skin and lungs (Mohammadi et al., 2019; Khan et al., 2023). For the dermal route, all samples for children and 97.8% of samples for adults indicated a moderate carcinogenic risk. Calculated *TCR* values ranged from  $1.1\text{E-}04$  to  $2.8\text{E-}03$ , with a mean value of  $1.6\text{E-}03$  for children, and from  $7.5\text{E-}05$  to  $1.9\text{E-}03$ , with a mean value of  $1.1\text{E-}03$  for adults. According to the results, 97.8% of samples for children and 28.9% for adults were deemed hazardous, indicating a very high risk of cancer. The spatial distribution of *TCR* shows that almost all groundwater samples in the study area present high to very high carcinogenic health risks (Figure 4). Numerous studies have also noted the high carcinogenic risks associated with dermal and oral exposure to groundwater around the world, including in Iran (Mohammadi et al., 2019), India (Ahamad et al., 2020), Iran (Shams et al.,

2020), Morocco (Bouaissa et al., 2022), Egypt (Abdelhalim et al., 2023), Pakistan (Khan et al., 2023), and China (Han et al., 2023).

**Pollution source identification**

*Pearson correlation matrix*

The PCM can be used to examine the relationships between variables and determine their origins in groundwater. Correlation coefficient values varied from +1 to -1, where +1 denotes a strong positive correlation and -1 a strong negative correlation. A coefficient of 0 indicates that the variables are not correlated (Shil and Singh, 2019). Figure 5 show the Pearson correlation matrix with a significant level of  $p < 0.05$ . The variables pH, EC, As, Cr, Cu, Ni, Pb and Zn show

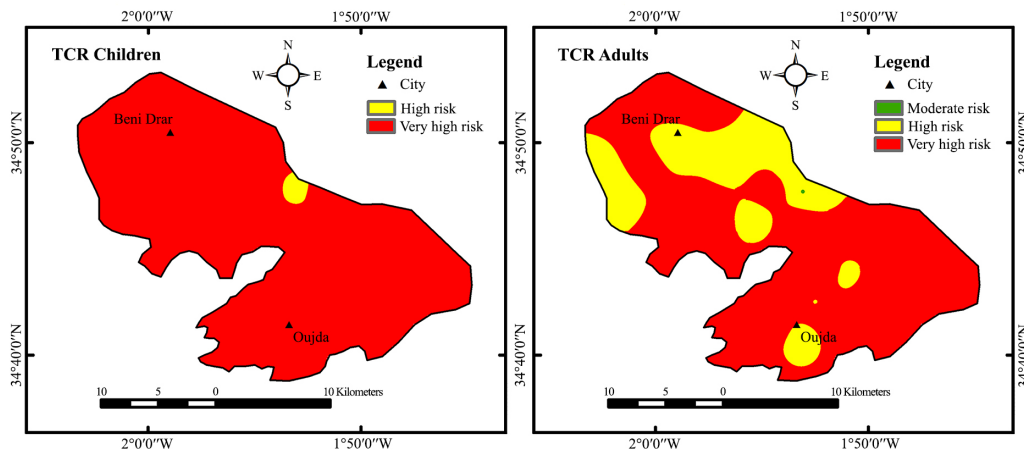


Figure 4. Distribution spatial of TCR

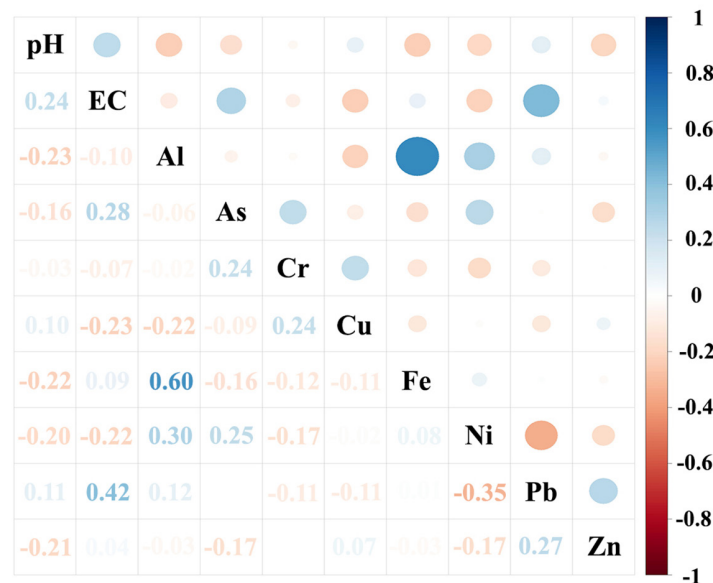


Figure 5. Pearson correlation chart of the analyzed parameters

**Table 8.** PCA for physicochemical and heavy metals

Specification	PC1	PC2	PC3	PC4	PC5
pH	-0.544	0.035	0.079	-0.570	0.375
EC	-0.370	0.618	0.487	0.032	0.091
Al	0.744	0.380	-0.057	0.090	0.318
As	0.005	-0.116	0.829	0.420	-0.063
Cr	-0.178	-0.339	0.082	0.628	0.318
Cu	-0.226	-0.490	-0.361	0.182	0.542
Fe	0.628	0.455	-0.161	0.004	0.403
Ni	0.637	-0.315	0.325	-0.114	-0.232
Pb	-0.339	0.730	-0.031	0.185	0.003
Zn	-0.156	0.278	-0.492	0.520	-0.421
Eigen value	2.007	1.812	1.446	1.255	1.043
% of variance	20.068	18.120	14.457	12.547	10.429
Cumulative %	20.068	38.188	52.645	65.192	75.621

no correlation with the other variables. Whereas a moderate correlation was noted between Al and Fe. The correlation suggests that Al and Fe come from similar sources, whether of geogenic origin or resulting from anthropogenic activities (Rajmohan et al., 2022).

#### Principal component analysis

PCA was used to identify potential sources of toxic metals in groundwater. A total of 10 variables for 24 samples were considered. Eigenvalues, percentage variance and cumulative percentage are presented in Table 8. PCA divided the data into five principal components (PC1 to PC5). PC1 accounted for the largest share of variance, 20%, with high positive loading of Al, Fe and Ni, suggesting that weathering of iron oxides/hydroxides and aluminum silicates is a predominant source of these metals (Rajmohan et al., 2022). These results corroborate those obtained by Pearson correlation. However, the positive loading of electrical conductivity (EC) and Pb in PC2, accounting for 18.1% of the total variance, indicates that other sources, such as the intensively evaporated infiltration of irrigation water from farmland, evaporite dissolution and evaporation, probably contribute to groundwater quality (Shil and Singh, 2019). As in PC3 (14.5% of variance) and Cu in PC5 (10.4% of variance) showed a positive correlation, indicating that they originate from distinct sources. PC4 explains 12.6% of the variance and shows a positive charge for Cr and Zn, while pH is negatively charged. The main sources of these metals may be of geogenic origin or derive from various anthropogenic activities.

## CONCLUSIONS

This study provides an assessment approach for characterizing and quantifying the sources, contamination levels and human health risks associated with heavy metals in groundwater in the Angads plain, Morocco. Based on mean levels in groundwater samples, metals are ranked in descending order of concentration: Fe > Al > As > Zn > Pb > Ni > Cr > Cu. The results indicate that almost all the heavy metals in the groundwater samples are below WHO guideline values, indicating that the water is not contaminated with metals and is safe for consumption. The estimated values of the heavy metal pollution index and the heavy metal evaluation index confirm that all groundwater samples are suitable for consumption due to their low metal load. Multivariate statistical analysis identified sources of water pollution, mainly attributable to anthropogenic activities. Non-carcinogenic risks by the cutaneous route were deemed safe for both populations studied, while by the oral route, the majority of groundwater presented risks to human health. This unique study will provide decision-makers with the information they need to implement monitoring strategies to effectively manage groundwater resources in the Angads plain.

## REFERENCES

1. Abdelhalim A., Howard G., Howden N.J.K., Ahmed M., Ismail E. 2023. Carcinogenic and non-carcinogenic health risk assessment of heavy metals contamination in groundwater in the west of Minia area, Egypt. *Human and Ecological Risk Assessment: An*

- International Journal, 29, 571-596. <https://doi.org/10.1080/10807039.2022.2153010>
2. Ahamad A., Raju N.J., Madhav S., Khan A.H. 2020. Trace elements contamination in groundwater and associated human health risk in the industrial region of southern Sonbhadra, Uttar Pradesh, India. *Environmental Geochemistry and Health*, 42, 3373-3391. <https://doi.org/10.1007/s10653-020-00582-7>
  3. Alshehri F., Almadani S., El-Sorogy A.S., Alwaq-dani E., Alfaifi H.J., Alharbi T. 2021. Influence of seawater intrusion and heavy metals contamination on groundwater quality, Red Sea coast, Saudi Arabia. *Marine Pollution Bulletin*, 165, 112094. <https://doi.org/10.1016/j.marpolbul.2021.112094>
  4. Aqil H., Khattach D., Gout R., El Mandour A., Olivier K. 2010. Contribution de la gravimétrie à la reconnaissance de l'aquifère profond de la plaine des Angad (Maroc nord-oriental). *Sécheresse*, 21, 252-256. <https://doi.org/10.1684/sec.2010.0247>
  5. Bangotra P., Jakhu R., Prasad M., Aswal R.S., Ashish A., Mushtaq Z., Mehra R. 2023. Investigation of heavy metal contamination and associated health risks in groundwater sources of southwestern Punjab, India. *Environmental Monitoring and Assessment*, 195, 367. <https://doi.org/10.1007/s10661-023-10959-7>
  6. Basraoui N. E., Ben-tahar R., Delière J.F., El Guerrouj B., Chafi A. 2024. Potentially toxic elements contamination and ecological risk assessment in surface sediments of Moulouya Estuary (Northeastern, Morocco). *Scientific African*, 25, e02295. <https://doi.org/10.1016/j.sciaf.2024.e02295>
  7. Biswas P., Hossain M., Patra P.K. 2023. Arsenic hydrogeochemistry, quality assessment, and associated health risks of groundwater through the novel water pollution index (WPI) and GIS approach. *Groundwater for Sustainable Development*, 21, 100944. <https://doi.org/10.1016/j.gsd.2023.100944>
  8. Bouaissa M., Gharibi E., Ghalit M., Taupin J. D., Boukich O., El Khattabi J. 2022. Groundwater quality evaluation using the pollution index and potential non-carcinogenic risk related to nitrate contamination in the karst aquifers of Bokoya massif, northern Morocco. *International Journal of Environmental Analytical Chemistry*, 1-21. <https://doi.org/10.1080/03067319.2022.2125308>
  9. Boughriba M., Barkaoui A., Zarhloule Y., Lahmer Z., Houadi B., Verdoya M. 2010. Groundwater vulnerability and risk mapping of the Angad transboundary aquifer using DRASTIC index method in GIS environment. *Arabian Journal of Geosciences*, 3, 207-220. <https://doi.org/10.1007/s12517-009-0072-y>
  10. Egbueri J.C. 2020. Heavy metals pollution source identification and probabilistic health risk assessment of shallow groundwater in Onitsha. *Anal Lett, Nigeria. Analytical Letters*, 53, 1620-1638. <https://doi.org/10.1080/00032719.2020.1712606>
  11. Gueddari H., Akodad M., Baghour M., Moumen A., Skalli A., Chahban M., Azizi G., Hmeid H. A., Maach M., Riouchi R., Yousfi Y. E. 2022. Assessment of potential contamination of groundwater in abandoned mining region of Ben Taieb, Northeastern Morocco using statistical studies. *International Journal of Health Sciences*, 6(S3), 412164133. <https://doi.org/10.53730/ijhs.v6nS3.6694>
  12. Gueddari H., Akodad M., Baghour M., Moumen A., Skalli A., El Yousfi Y., Ait Hmeid H., Chahban M., Azizi G., Rahhou A., Ahmed I., Muhammad Z. 2021. Assessment of the metal contamination index in groundwater of the quaternary of the Middle Kert Basin, north-eastern Morocco. *Environmental Quality Management*, 32, 1, 53-62. <https://doi.org/10.1002/tqem.21824>
  13. Han W., Pan Y., Welsch E., Liu X., Li J., Xu S., Peng H., Wang F., Li X., Shi H., Chen W., Huang C. 2023. Prioritization of control factors for heavy metals in groundwater based on a source oriented health risk assessment model. *Ecotoxicology and Environmental Safety*, 267, 115642. <https://doi.org/10.1016/j.ecoenv.2023.115642>
  14. Khalid S., Shahid M., Natasha., Shah A. H., Saeed F., Ali M., Qaisrani S. A., Dumat C. 2020. Heavy metal contamination and exposure risk assessment via drinking groundwater in Vehari, Pakistan. *Environmental Science and Pollution Research*, 27, 39852-39864. <https://doi.org/10.1007/s11356-020-10106-6>
  15. Khan Y.K., Toqeer M., Shah M.H. 2023. Characterization, Source Apportionment and Health Risk Assessment of Trace Metals in Groundwater of Metropolitan Area in Lahore, Pakistan. *Exposure and Health*, 15, 915-931. <https://doi.org/10.1007/s12403-022-00531-y>
  16. Kim J.J., Kim Y.S., Kumar V. 2019. Heavy metal toxicity: an update of chelating therapeutic strategies. *Journal of Trace Elements in Medicine and Biology*, 54, 226-231. <https://doi.org/10.1016/j.jtemb.2019.05.003>
  17. Lahrach A., Zarhloule Y., Azhimi M., El boumashouli S. M., Jabrane R., Dsouli K., Halouani H. 2006. The Angads aquifer (Eastern Morocco): flow modelling and management perspectives. *Geomaghreb*, 3, 23-34.
  18. Lotfi S., Chakit M., Belghyti D. 2020. Groundwater Quality and Pollution Index for Heavy Metals in Saïs Plain, Morocco. *Journal of Health and Pollution*, 10(26), 200603. <https://doi.org/10.5696/2156-9614-10.26.200603>
  19. Mahjoub M., Ben-Tahar R., Omari A., Arabi M., Boukich O., Slamini M., Smiri Y. 2024. Hg, Cd, and Pb in fish of the Moulouya River, Morocco, and human health risk. *Food Additives & Contaminants: Part B*, 1-10. <https://doi.org/10.1080/19393210.2024.2367476>

20. Masoud M.H.Z., Rajmohan N., Basahi J.M., Niyazi B.A.M. 2022. Application of water quality indices and health risk models in the arid coastal aquifer, Southern Saudi Arabia. *Environmental Science and Pollution Research*, 29, 70493-70507. <https://doi.org/10.1007/s11356-022-20835-5>
21. Mohammadi A.A., Zarei A., Majidi S., Ghaderpoury A., Hashempour Y., Saghi M.H., Alinejad A., Yousefi M., Hosseingholizadeh N., Ghaderpoori M. 2019. Carcinogenic and non-carcinogenic health risk assessment of heavy metals in drinking water of Khorramabad, Iran. *MethodsX*, 6, 1642-1651. <https://doi.org/10.1016/j.mex.2019.07.017>
22. Mthembu P.P., Elumalai V., Li P., Uthandi S., Rajmohan N., Chidambaram S. 2022. Integration of heavy metal pollution indices and health risk assessment of groundwater in semi-arid coastal aquifers, South Africa. *Exposure and Health*, 14, 487-502. <https://doi.org/10.1007/s12403-022-00478-0>
23. Moulouya Water Basin Agency. 2023. Directorate General of Hydraulics, Ministry of Equipment and Water, Kingdom of Morocco.
24. Nayak S.K., Nandimandalam J.R. 2023. Impacts of climate change and coastal salinization on the environmental risk of heavy metal contamination along the Odisha coast, India. *Environmental Research*, 238, 117175. <https://doi.org/10.1016/j.envres.2023.117175>
25. Rajmohan N., Niyazi B.A.M., Masoud M.H.Z. 2022. Trace metals pollution, distribution and associated health risks in the arid coastal aquifer, Hada Al-Sham and its vicinities Saudi Arabia. *Chemosphere*, 297, 134246. <https://doi.org/10.1016/j.chemosphere.2022.134246>
26. Ren X., Li P., He X., Su F., Elumalai V. 2021. Hydrogeochemical processes affecting groundwater chemistry in the central part of the Guanzhong basin, China. *Archives of Environmental Contamination and Toxicology*, 80, 74-91. <https://doi.org/10.1007/s00244-020-00772-5>
27. Rezaei A., Hassani H., Hassani S., Jabbari N., Mousavi S.B.F., Rezaei S. 2019. Evaluation of groundwater quality and heavy metal pollution indices in Bazman basin, southeastern Iran. *Groundwater for Sustainable Development*, 9, 100245. <https://doi.org/10.1016/j.gsd.2019.100245>
28. General Population and Housing Census. 2014. Population census, high planning commission, Kingdom of Morocco.
29. Royal Institute for Strategic Studies. 2022. The future of water in Morocco? Summary report of the scientific day's work, Kingdom of Morocco.
30. Shams M., Nezhad N.T., Dehghan A., Alidadi H., Paydar M., Mohammadi A.A., Zarei A. 2020. Heavy metals exposure, carcinogenic and non-carcinogenic human health risks assessment of groundwater around mines in Joghatai, Iran. *International Journal of Environmental Analytical Chemistry*, 102(8), 1884-1899. <https://doi.org/10.1080/03067319.2020.1743835>
31. Sharma K., Janardhana Raju N., Singh N., Sreekesh S. 2022. Heavy metal pollution in groundwater of urban Delhi environs: pollution indices and health risk assessment. *Urban Climate*, 45, 101233. <https://doi.org/10.1016/j.uclim.2022.101233>
32. Shil S., Singh U.K. 2019. Health risk assessment and spatial variations of dissolved heavy metals and metalloids in a tropical river basin system. *Ecological Indicators*, 106, 105455. <https://doi.org/10.1016/j.ecolind.2019.105455>
33. Singh K.R., Dutta R., Kalamdhad A.S., Kumar B. 2020. Review of existing heavy metal contamination indices and development of an entropy-based improved indexing approach. *Environment, Development and Sustainability*, 22, 7847-7864. <https://doi.org/10.1007/s10668-019-00549-4>
34. United States Environmental Protection Agency. 2011. Exposure Factors Handbook 2011 Edition (Final); United States Environmental Protection Agency: Washington, DC, USA.
35. United States Environmental Protection Agency. 2014. Human Health Evaluation Manual, Supplemental Guidance: Update of Standard Default Exposure Factors-OSWER Directive 9200.
36. Usman U.A., Yusoff I., Raoov M., Hodgkinson J. 2020. Trace metals geochemistry for health assessment coupled with adsorption remediation method for the groundwater of Lorong Serai 4, Hulu Langat, west coast of Peninsular Malaysia. *Environmental Geochemistry and Health*, 42, 3079-3099. <https://doi.org/10.1007/s10653-020-00543-0>
37. Wagh V.M., Panaskar D.B., Mukate S.V., Gaikwad S.K., Muley A.A., Varade A.M. 2018. Health risk assessment of heavy metal contamination in groundwater of Kadava River Basin, Nashik, India. *Modeling Earth Systems and Environment*, 4, 969-980. <https://doi.org/10.1007/s40808-018-0496-z>
38. World Health Organization. 2017. Guidelines for Drinking Water Quality: Fourth Edition Incorporating the First Addendum. World Health Organization, Geneva.
39. Yuan B., Cao H., Du P., Ren J., Chen J., Zhang H., Zhang Y., Luo H. 2023. Source-oriented probabilistic health risk assessment of soil potentially toxic elements in a typical mining city. *Journal of Hazardous Materials*, 443, 130222. <https://doi.org/10.1016/j.jhazmat.2022.130222>
40. Zarhloule Y., Boughriba M., Barkaoui A., Chanioui M. 2010. Water as parameter of cooperation between Morocco and Algeria the case of trans-boundary stressed aquifers of Bounaïm-Tafna basin. *AQUAMundi journal*, 1, 73-78. <https://doi.org/10.4409/Am-011-10-001>